DOI: 10.1534/genetics.106.069732

Inorganic Phosphate Deprivation Causes tRNA Nuclear Accumulation via Retrograde Transport in *Saccharomyces cerevisiae*

Rebecca L. Hurto,* Amy Hin Yan Tong,† Charles Boone† and Anita K. Hopper*,[1]

**Department of Molecular Genetics, Ohio State University, Columbus, Ohio 43210 and †Banting and Best Department of Medical Research, University of Toronto, Toronto, Ontario M5G 1L6, Canada*

Manuscript received January 21, 2007
Accepted for publication March 12, 2007

ABSTRACT

Nuclear export of tRNA is an essential eukaryotic function, yet the one known yeast tRNA nuclear exporter, Los1, is nonessential. Moreover recent studies have shown that tRNAs can move retrograde from the cytosol to the nucleus by an undefined process. Therefore, additional gene products involved in tRNA nucleus–cytosol dynamics have yet to be identified. Synthetic genetic array (SGA) analysis was employed to identify proteins involved in Los1-independent tRNA transport and in regulating tRNA nucleus–cytosol distribution. These studies uncovered synthetic interactions between *los1*Δ and *pho88*Δ involved in inorganic phopshate uptake. Further analysis revealed that inorganic phosphate deprivation causes transient, temperature-dependent nuclear accumulation of mature cytoplasmic tRNA within nuclei via a Mtr10- and retrograde-dependent pathway, providing a novel connection between tRNA subcellular dynamics and phosphate availability.

TRANSPORT of tRNA from its nuclear site of biogenesis to the cytosol is an essential eukaryotic process as tRNA must be available for translation, which occurs in the cytosol. Intracellular tRNA movement in the budding yeast *Saccharomyces cerevisiae* involves several steps. First, end-matured pre-tRNAs are transported from nucleus to cytosol ("primary tRNA nuclear export"). Once in the cytosol, pre-tRNAs containing introns are spliced by the splicing endonuclease complex located on the cytosolic surface of the mitochondrial outer membrane (Yoshihisa *et al.* 2003). Numerous nucleoside modification steps also occur in the nucleus and cytosol (Hopper and Phizicky 2003). Mature cytosolic tRNA are then available for translation. Recent work demonstrated that mature tRNA can move from cytosol to nucleus (Shaheen and Hopper 2005; Takano *et al.* 2005) and vice versa ("re-export"; Whitney *et al.* 2007). However, many of the gene products involved in the tRNA nucleus-to-cytosol and cytosol-to-nucleus transport pathways have yet to be defined.

Transport of many macromolecules between the nucleus and the cytosol requires the small GTPase, Ran, and its protein-binding partners, the β-importins. Ran is maintained in the GTP-bound state in nuclei by *Ran g*uanosine *e*xchange *f*actor (RanGEF), which is encoded in yeast by *PRP20* and resides in the nucleus. β-Importin family members that export cargo from the nucleus to the cytosol bind their cargo only in the presence of RanGTP and then mediate interactions with the nuclear pore complexes to allow the entire complex to move to the cytosol. Once in the cytosol, RanGTP interacts with the *Ran G*TPase *a*ctivating *p*rotein (RanGAP), encoded by *RNA1*, which activates GTP hydrolysis, leading to conformational changes that cause the heterotrimeric complexes to dissociate, releasing the cargo in the cytosol (Corbett *et al.* 1995; Gorlich and Kutay 1999; Weis 2003). For tRNA nuclear export, Los1, a member of the β-importin family, binds tRNA in a RanGTP-dependent manner (Hellmuth *et al.* 1998). The mammalian homolog of Los1, Exportin-t (Xpo-t), has also been shown to bind end-processed tRNA, with or without introns, as part of a heterotrimeric complex with RanGTP (Arts *et al.* 1998a,b; Kutay *et al.* 1998).

Inhibiting the Los1-dependent tRNA transport pathway through a temperature-sensitive mutation of *RNA1* (*rna1-1*) or mutation of *LOS1* caused nuclear accumulation of tRNA (Sarkar and Hopper 1998). Similarly, blocking Xpo-t-mediated tRNA transport through microinjection of Xpo-t antibodies in Xenopus oocytes reduced nuclear export of $tRNA^{Phe}$ by 99% (Arts *et al.* 1998b). Blocking transport through mutation of *RNA1*, *PRP20*, *LOS1*, or some nucleopore genes also caused accumulation of intron-containing pre-tRNA (Hopper *et al.* 1978, 1980; Kadowaki *et al.* 1993; Sharma *et al.* 1996), which indicated that these proteins were involved in the transport of end-matured pre-tRNA to the cytosol.

Numerous mutations have been identified that affect tRNA nucleus–cytosol distribution without causing accumulation of intron-containing pre-tRNA. These

[1]*Corresponding author:* Department of Molecular Genetics, Ohio State University, 484 W. 12th Ave., Columbus, OH 43210.
E-mail: hopper.64@osu.edu

include temperature-sensitive mutations of methionyl- (*mes1-1*), isoleucyl- (*ils1-1*), and tyrosyl- (*tys1-1*) aminoacyl-tRNA synthetases (Sarkar *et al.* 1999), 3′ tRNA CCA-nucleotidyl transferase (*cca1-1*; Grosshans *et al.* 2000; Feng and Hopper 2002), and the *tef1*Δ *tef2-1* double mutation of the eukaryotic elongation factor 1A (Grosshans *et al.* 2000). Lack of intron-containing pre-tRNA accumulation indicates that tRNA nuclear accumulation observed in these mutants occurs via accrual of fully processed, mature tRNA from the cytosol, and not by inhibition of the primary tRNA nuclear export pathway that exports pre-tRNA to the cytosol.

One genetic approach for defining parallel pathways that accomplish essential cellular functions is the identification of new mutations that have synthetic interactions with known mutations that impair or block one of the pathways. As tRNA nuclear export is an essential process and *LOS1* is a known nonessential nuclear exporter of tRNA (Hurt *et al.* 1987), this approach should be useful for the identification of genes that encode proteins participating in Los1-independent transport of end-matured pre-tRNA and mature tRNA and, possibly, negative regulators of tRNA retrograde transport.

Previous work employing standard synthetic lethal methodology identified several synthetic interactions with *los1*Δ. The genes identified affected a variety of cellular processes, including tRNA aminoacylation (Simos *et al.* 1996a), tRNA modification (Simos *et al.* 1996a), Pol III transcription (Simos *et al.* 1996b), and translation (Hellmuth *et al.* 1998; Grosshans *et al.* 2000). *S*ynthetic *g*enetic *a*rray (SGA) analysis (Tong *et al.* 2001) allows extensive, large-scale, systematic searches for genetic interactions. This approach was utilized with a collection of promoter replacement alleles of essential genes and *los1*Δ (Davierwala *et al.* 2005). Depletion of Taf3, a subunit of the Pol II transcription initiation complex, and depletion of Pop5, a subunit of both RNase MRP (pre-rRNA cleavage) and RNase P (pre-tRNA 5′-end processing), were found to have synthetic interactions with *los1*Δ (Davierwala *et al.* 2005). None of the previously reported studies have identified tRNA nuclear exporters that function in parallel to Los1 or regulators of tRNA nucleus–cytosol distribution.

Here, we describe the results of SGA screens of *los1*Δ using the yeast *MAT***a** deletion collection. Novel synthetic interactions were observed between *los1*Δ and *snt309*Δ, *aro7*Δ, *rpl12a*Δ, *rpl13b*Δ, *lrp1*Δ, *gtr1*Δ, *gtr2*Δ, or *pho88*Δ. Of these verified candidates, *gtr1*Δ, *gtr2*Δ, and *pho88*Δ caused tRNA nuclear accumulation. As *gtr1*Δ, *gtr2*Δ, and *pho88*Δ have been previously shown to influence inorganic phosphate (P_i) uptake (Bun-Ya *et al.* 1992; Yompakdee *et al.* 1996; Lagerstedt *et al.* 2005), we examined the affect of P_i starvation upon tRNA nucleus–cytosol distribution. Transient, temperature-dependent, tRNA nuclear accumulation was observed in wild-type cells grown on synthetic media lacking P_i for 1–2 hr at 23° or 30°. Northern and heterokaryon analyses of P_i-deprived cells and of *pho88*Δ cells indicated that the observed nuclear accumulation was due to accrual of mature tRNA, which entered the nucleus via retrograde transport. This work provides a novel connection between P_i availability and tRNA nucleus–cytosol distribution.

MATERIALS AND METHODS

Strains and media: *Strains:* Yeast strains used for these studies are listed in Table 1. All plasmid transformations were made by lithium acetate (LiOAc) transformation (Schiestl and Gietz 1989). Deletions were accomplished by LiOAc transformation of the parent yeast strain with a PCR product cassette that replaced the endogenous gene. Sequences for the oligonucleotides used are listed in supplemental Table S1 at http://www.genetics.org/supplemental/. The *los1::natMX4* cassette was generated by PCR amplification using oligonucleotide primers RLH007A and RLH007B and a *natR-MX4* template (p4339; Tong *et al.* 2001). LOS1KO1B was derived from the transformation of Y3656 with the *los1::natMX4* cassette. The deletion of *LOS1* was verified using the primers RLH010A and RLH010B. The *pho88::natMX4* cassette was generated by PCR amplification using oligonucleotide primers RLH017A and RLH017B and a natR-MX4 template (Goldstein and McCusker 1999). 8MS88ΔN2C was derived from the transformation of MS739 with the *pho88::natMX4* cassette. BY*88*ΔF1 was derived from the transformation of BY4741 with the *pho88::natMX4* cassette. The *pho88::hphMX4* cassette was generated by PCR amplification using the oligonucleotide primers RLH017A and RLH017B and the hphR-MX4 template (Goldstein and McCusker 1999). BY88ΔD1 and BY88ΔG4 were derived from independent transformations of BY4741 with the *pho88::hphMX4* cassette. 8MS88ΔH2D was derived from the transformation of MS739 with the *pho*88*::hphMX4* cassette. YD05055 (*los1::kanMX*) was transformed with YCp*LOS1* (Hurt *et al.* 1987) and then with the *pho*88*::hphMX4* cassette to form strain *los1*Δ *pho88*Δ + YCp*LOS1*. The deletion of *PHO88* was verified using primers RLH017C, RLH017D, and RLH017E. The strain *los1*Δ *pho88*Δ + YCp*LOS1* was grown on nonselective media to allow plasmid loss from which *los1*Δ *pho88*Δ was derived.

Media: Yeast strains were maintained on YEPD [*y*east *e*xtract, trypticase *p*eptone, *d*extrose, supplemented with adenine (0.04 g/liter), uracil (0.04 g/liter)] medium; SC (*s*ynthetic *c*omplete) defined medium; Difco yeast nitrogen base without amino acids (6.7 g/liter; Becton Dickinson, Sparks, MD) supplemented with amino acids, dextrose (2%), adenine (0.04 g/liter), and uracil (0.04 g/liter). SC–P_i liquid medium is synthetic defined medium lacking K_2PO_4 [the source of P_i in SC; yeast nitrogen base lacking amino acids and K_2PO_4 (5.7 g/liter; ForMedium, Norwich, UK) supplemented with amino acids, uracil, and 1.0 g/liter KCl]. Solid YEPD medium supplemented with 2 g/liter KH_2PO_4 (Fisher) was utilized for the "wild-type" heterokaryon fluorescence *in situ* hybridization (FISH) analysis. To select for *natMX* cassette integration, the strains were grown on YEPD + clonNAT (100 mg/liter; Werner BioAgents, Jena, Germany) solid medium. To select for *hphMX* cassette integration, the strains were grown on YEPD + hygromycin B (300 mg/liter; Calbiochem, La Jolla, CA) solid medium.

Genetic analysis: SGA was performed and scored as previously described (Tong *et al.* 2001) using LOS1KO1B as the bait strain. The final replica plates were grown at 22° or 37°. Tetrad dissection was done by standard procedures.

Growth assay: Serial dilutions were made of the indicated yeast cultures. Aliquots (5 μl) of each dilution were spotted onto each plate of the indicated solid medium. The plates

TABLE 1

Yeast strains employed

Strain(s)	Genotype	Source
Y3656	*MAT*α *can1*Δ*::MFA1pr-HIS3-MF*α*1pr-LEU2 his3*Δ*1 leu2*Δ*0 lys2*Δ*0 ura3*Δ*0*	Tong *et al.* (1999)
LOS1KO1B	*MAT*α *can1*Δ*:MFA1pr-HIS3-MF*α*1pr-LEU2 his3*Δ*1 leu2*Δ*0 los1::natMX4 lys2*Δ*0 ura3*Δ*0*	This study
BY4741	*MAT***a** *his3*Δ*1 leu2*Δ*0 met15*Δ*0 ura3*Δ*0*	Open Biosystems (Huntsville, AL)
*MAT***a** deletion collection	*MAT***a** *orf::kanMX his3*Δ*1 leu2*Δ*0 met15*Δ*0 ura3*Δ*0 TRP1 LYS2*	Winzeler *et al.* (1999); Open Biosystems
YD05055	*MAT***a** *los1::kanMX his3*Δ*1 leu2*Δ*0 met15*Δ*0 ura3*Δ*0 TRP1 LYS2*	*MAT***a** deletion collection
*los1*Δ*pho88*Δ	*MAT***a** *los1::kanMX pho88::hphMX his3*Δ*1 leu2*Δ*0 met15*Δ*0 ura3*Δ*0 TRP1 LYS2*	This study
*arc1*Δ*MAT***a**	*MAT***a** *arc1::kanMX his3*Δ*1 leu2*Δ*0 met15*Δ*0 ura3*Δ*0 TRP1 LYS2*	*MAT***a** deletion collection
*pho88*Δ*MAT***a**	*MAT***a** *pho88::kanMX his3*Δ*1 leu2*Δ*0 met15*Δ*0 ura3*Δ*0 TRP1 LYS2*	*MAT***a** deletion collection
*rpl13b*Δ*MAT***a**	*MAT***a** *rpl13b::kanMX his3*Δ*1 leu2*Δ*0 met15*Δ*0 ura3*Δ*0 TRP1 LYS2*	*MAT***a** deletion collection
*npr1*Δ*MAT***a**	*MAT***a** *npr1::kanMX his3*Δ*1 leu2*Δ*0 met15*Δ*0 ura3*Δ*0 TRP1 LYS2*	*MAT***a** deletion collection
BY88ΔD1	*MAT***a** *pho88::hphMX his3*Δ*1 leu2*Δ*0 met15*Δ*0 ura3*Δ*0 TRP1 LYS2*	This study
BY88ΔF1	*MAT***a** *pho88::natMX his3*Δ*1 leu2*Δ*0 met15*Δ*0 ura3*Δ*0 TRP1 LYS2*	This study
BY88ΔG4	*MAT***a** *pho88::hphMX his3*Δ*1 leu2*Δ*0 met15*Δ*0 ura3*Δ*0 TRP1 LYS2*	This study
BY4742	*MAT*α *his3*Δ*1 leu2*Δ*0 lys2*Δ*0 ura3*Δ*0*	Open Biosystems
*MAT*α deletion collection	*MAT*α *orf::kanMX his3*Δ*1 leu2*Δ*0 lys2*Δ*0 ura3*Δ*0*	Winzeler *et al.* (1999); Open Biosystems
MS739	*MAT*α *ade2-101 kar1-1 leu2-3,112 ura3-52*	M. Rose, Princeton University
MS739 + $tRNA^{GluD}$	*MAT*α *ade2-101 kar1-1 leu2-3,112 ura3-52* pRS416$tRNA^{Glu\text{-}D}$	Shaheen and Hopper (2005)
8MS88ΔN2C	*MAT*α *ade2-101 kar1-1 leu2-3,112 pho88::natMX4 ura3-52*	This study
8MS88ΔH2D	*MAT*α *ade2-101 kar1-1 leu2-3,112 pho88::hphMX4 ura3-52*	This study
8MS88ΔH2D + $tRNA^{GluD}$	*MAT*α *ade2-101 kar1-1 leu2-3,112 pho88::hphMX4 ura3-52* pRS416$tRNA^{Glu\text{-}D}$	This study

were incubated for 2–3 days at the indicated temperature. Images of the plates were captured using Eagle Eye II (Stratagene, La Jolla, CA), digital camera, or scanner (ScanMaker 8700 by Microtek, Carson, CA). Adobe Photoshop 5.0 was used for image assembly.

Fluorescence *in situ* hybridization: FISH was performed as previously described (Sarkar and Hopper 1998) with the modifications detailed in Stanford *et al.* (2004). Heterokaryons for FISH were mated and grown as described in Shaheen and Hopper (2005) except the solid YEPD medium used for the "wild-type" mating was medium supplemented with 2 g/liter KH_2PO_4 (Fisher) to prevent premature induction of the *PHO* pathway, as low levels of *PHO5* expression have been observed when cells are grown in YEPD medium (Yoshida *et al.* 1989a,b). Oligonucleotides used as probes are listed in supplemental Table S1 at http://www.genetics.org/supplemental/. Each slide contained positive and negative controls for tRNA nuclear accumulation. When adjectives describing the relative amount of tRNA nuclear accumulation are used, the probes were hybridized under the same conditions. All critical experiments were independently viewed and scored by at least two people, one of whom was unaware of the experimental details. A Nikon Microphot-FX microscope was used to observe fluorescence and a Sensys charge-coupled device camera (Photometrics, Tucson AZ) using QED software (QED Imaging, Pittsburgh) was used to capture the images. Adobe Photoshop 5.0 was used for image assembly.

Northern analysis: Small RNAs were extracted from yeast cultures grown to densities similar to those used for FISH as previously described (Hopper *et al.* 1980). Samples (10 μg of RNA) were electrophoretically separated at 4° in 10% polyacrylamide gel containing 8 M urea and 1× TBE (0.09 M Tris, 0.09 M borate, 0.001 M ethylenediaminetetraacetic acid). RNAs were electrophoretically transferred onto Hybond N+ membranes (Amersham Pharmacia) using a Hoefer TE42 Transphor apparatus (Hoefer Scientific) filled with 1× TAE buffer (40 mM Tris, 20 mM acetate, 1 mM EDTA). Membranes were prehybridized at 37° in 4× SSC (1× is 0.15 M NaCl, 0.015 M sodium citrate), 2.5× Denhart's solution [1× is 0.02% Ficoll (type 400), 0.02% polyvinylpyrrolidone, 0.02% bovine serum albumin], 50 μg/ml single-stranded salmon sperm DNA, and 0.05% sodium dodecyl sulfate. Probe hybridization was at 37° in the same buffer with the addition of oligonucleotide probes (supplemental Table S1 at http://www.genetics.org/supplemental/) that were 5′ end labeled with [^{32}P]ATP using T4 polynucleotide kinases (Promega, Madison, WI). After hybridization, membranes were UV crosslinked, washed in 2× SSC, and used to expose Kodak BioMax MS film (Eastman Kodak, Rochester, NY).

Acid phosphatase assay: Acid phoshatase activity was determined as previously described (Byrne *et al.* 2004) except that yeast cultures were grown to early log phase and the volume of cells was increased to compensate for the reduced number of cells.

RESULTS

SGA analysis of *los1*Δ uncovers eight novel interactions: SGA was performed twice using LOS1KO1B (*los1::nat*^{R}) as bait. All of the incubation steps for the first screen were conducted at 22°, the standard temperature for SGA. The final replica plates of the second screen were incubated at 37°, a temperature that exaggerates the *los1*Δ phenotype in some strains (Hopper

TABLE 2

***Bona fide los1*Δ interactions**

ORF	Gene	Interaction	tRNA distribution
YGL105W	*ARC1*	Lethal	Nuclear accumulation/ even distribution[a]
YPR101W	*SNT309*	Enhanced growth	Not determined
YPR060C	*ARO7*	Slow growth	Not determined
YEL054C	*RPL12A*	Slow growth	Even distribution
YMR142C	*RPL13B*	Slow growth	Even distribution
YHR081W	*LRP1*	Slow growth	Not determined
YML121W	*GTR1*	Slow growth	Nuclear accumulation
YGR163W	*GTR2*	Slow growth	Nuclear accumulation
YBR106W	*PHO88*	Lethal/slow growth	Nuclear accumulation

[a] Nuclear accumulation of $tRNA^{Met}$, even distribution of $tRNA^{Tyr}$ and $tRNA^{Ile}$.

et al. 1980). The first screen provided 18 novel candidate interactions, whereas the second screen uncovered 118 candidates. As only six candidates appeared in both screens—deletions of *ARC1* (*YGL105W*), *LDB16* (*YCL005W*), *LRP1* (*YHR081W*), *RCY1* (*YJL204C*), *WHI3* (*YNL197C*), and *RPL13B* (*YMR142C*)—the total number of candidates was 131 (supplemental Table S2 at http://www.genetics.org/supplemental/). Candidates of the first screen did not necessarily overlap with the candidates found in the second screen, possibly due to changes in the phenotype of individual deletion strains at different temperatures, manipulation errors, false positives, or false negatives. *ARC1*, a known synthetic lethal interaction (Simos *et al.* 1996b), was found in both screens, indicating that the assay was functioning as predicted.

Tetrad analysis and growth assays of selected haploid progeny were utilized to detect and verify synthetic lethal, slow, or enhanced growth interactions. Tetrad analysis of 97 candidate interactions revealed eight *bona fide los1*Δ interactions (Table 2); only three of these appeared as candidates in both searches. Synthetic enhanced growth interaction was observed between *los1*Δ and *snt309*Δ (*YPR101W*). Synthetic slow-growth interactions were observed between *los1*Δ and *aro7*Δ (*YPR060C*), *rpl12a* (*YEL054C*), *rpl13b*Δ (*YMR142C*), *lrp1*Δ (*YHR081W*), *gtr1*Δ (*YML121W*), or *gtr2*Δ (*YGR163W*).

A synthetic lethal interaction between *los1*Δ and *pho88*Δ (*YBR106W*) was documented upon tetrad dissection at 23° by the absence of nonparental ditypes and the absence of *los1*Δ *pho88*Δ containing progeny in tetratype asci as predicted by two-gene synthetic lethality (Figure 1A). However, we were able construct a viable *los1*Δ *pho88*Δ strain via direct mutagenesis (see materials and methods). The *los1*Δ *pho88*Δ strain exhibited slower growth at 23° than strains containing either individual mutation (Figure 1B). The slow growth *vs.* synthetic lethal interactions observed between *los1*Δ and *pho88*Δ are addressed in the discussion.

SGA analysis uncovered genes influencing tRNA nucleus–cytosol distribution: The subcellular distributions of tRNA between the nucleus and the cytosol of selected synthetic interactors were evaluated using fluorescence *in situ* hybridization (Sarkar and Hopper 1998). Gene deletions that had synthetic slow-growth phenotypes were expected to cause tRNA nuclear accumulation if the growth defect was due to impairment of tRNA export. Nuclear accumulation of both $tRNA^{Met}$ and $tRNA^{Tyr}$, as indicated by the increased FITC signal that colocalizes with the DAPI-stained DNA, was observed in *los1*Δ (Figure 2A, column 2), *pho88*Δ (Figure 2A, column 5), *gtr1*Δ (supplemental Figure S1 at http://www.genetics.org/supplemental/ and data not shown), and *gtr2*Δ (supplemental Figure S1 at http://www.genetics.org/supplemental/ and data not shown) strains (Table 2). Several independent *pho88*Δ strains were generated, and

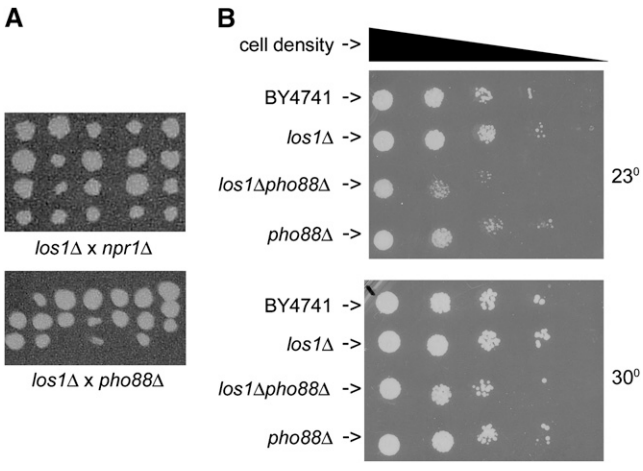

Figure 1.—Analysis of spore viability and growth of cells with *PHO88* and/or *LOS1* deletions. (A) Tetrad dissection of *los1*Δ (LOS1KO1B) × *pho88*Δ (*pho88*Δ*MAT***a**) and of *los1*Δ (LOS1KO1B) × *npr1*Δ (*npr1*Δ*MAT***a**) on YEPD. (B) BY4741, YD05055 (*los1*Δ *MAT***a**), *los1*Δ*pho88*Δ, and *pho88*Δ *MAT***a** were grown to saturation, and then equal amounts of cells from each strain were used to make two series of dilutions. Aliquots (5 μl) of each dilution were placed on solid synthetic complete medium. Plates were incubated for 2 days at the indicated temperatures.

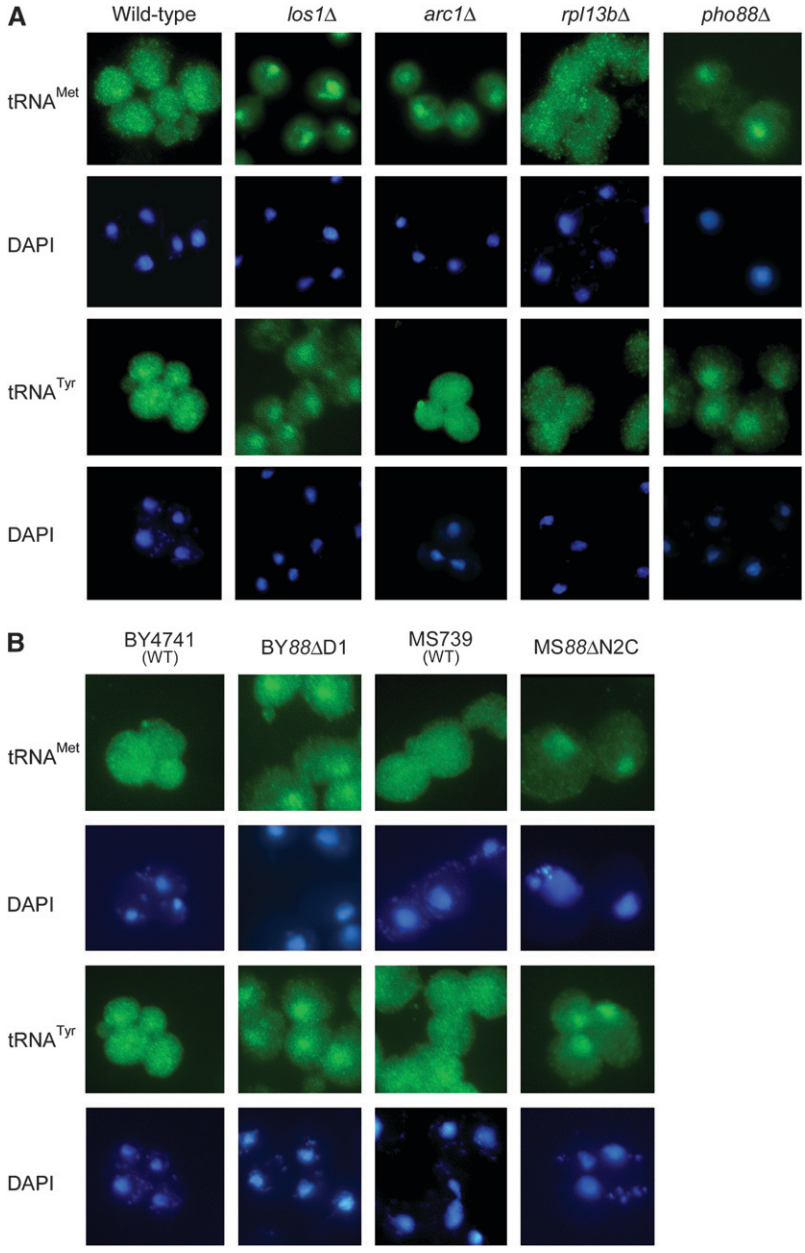

FIGURE 2.—Subcellular distribution of tRNA in selected SGA candidate deletions. (A) Location of tRNA within candidate deletion strains identified by SGA was determined by FISH analysis of BY4741 (wild type), YD05055 (*los1*Δ), *arc1*Δ*MAT***a**, *rpl13b*Δ*MAT***a**, and *pho88*Δ*MAT***a** cells. (Row 1) $tRNA^{Met}$; (row 3) $tRNA^{Tyr}$; (rows 2 and 4) DAPI stain of row 1 and 3 cells, respectively. (B) FISH analysis of BY4741 (wild type), BY88ΔD1 (*pho88::hph*^{R} in BY4741), MS739 (*kar1-1*), and 8MS88ΔN2C (*pho88::nat*^{R} in MS739) cells. (Row 1) $tRNA^{Met}$. (Row 3) $tRNA^{Tyr}$. (Rows 2 and 4) DAPI stain of row 1 and row 3 cells, respectively.

all exhibited tRNA nuclear accumulation (Figure 2B, columns 2 and 4; also see supplemental Figure S1 at http://www.genetics.org/supplemental/). In contrast, *arc1*Δ cells exhibited nuclear accumulation of $tRNA^{Met}$ while the cellular distribution of $tRNA^{Tyr}$ was similar to wild-type cells (Figure 2A, column 3). Deletion of *arc1*Δ influencing the nucleus–cytosol distribution of $tRNA^{Met}$, but not $tRNA^{Tyr}$, is consistent with the function of Arc1 as a cofactor of the methionyl- and glutamyl-tRNA synthetases (SIMOS *et al.* 1996a). However, not all deletions that had synthetic slow-growth interactions with *los1*Δ caused tRNA nuclear accumulation. For example, wild-type, *rpl13b*Δ, and *rpl12a*Δ cells had a similar cellular distribution of $tRNA^{Met}$ and $tRNA^{Tyr}$ (Figure 2A, columns 1 and 4, and supplemental Figure S1 at http://www.genetics.org/supplemental/, respectively; Table 2).

Candidate deletions that caused tRNA nuclear accumulation had been implicated in uptake of P_i. Gtr1 and Gtr2 formed a small GTPase complex (NAKASHIMA *et al.* 1999) that negatively regulated the Ran cycle (NAKASHIMA *et al.* 1996) and was required for efficient P_i uptake in response to P_i starvation (BUN-YA *et al.* 1992; LAGERSTEDT *et al.* 2005). Deletion of *PHO88* caused impaired P_i uptake and slowed growth (YOMPAKDEE *et al.* 1996). *PHO88* was selected for further study because it had strong synthetic interactions with *los1*Δ, its deletion caused tRNA nuclear accumulation, and it has been shown to impact the regulation of the *PHO* pathway (YOMPAKDEE *et al.* 1996).

P_i deprivation of wild-type cells caused tRNA nuclear accumulation: We obtained a plasmid encoding an N-terminal GST-tagged Pho88 (MARTZEN *et al.* 1999) and found that GST-Pho88 was located in the endoplasmic

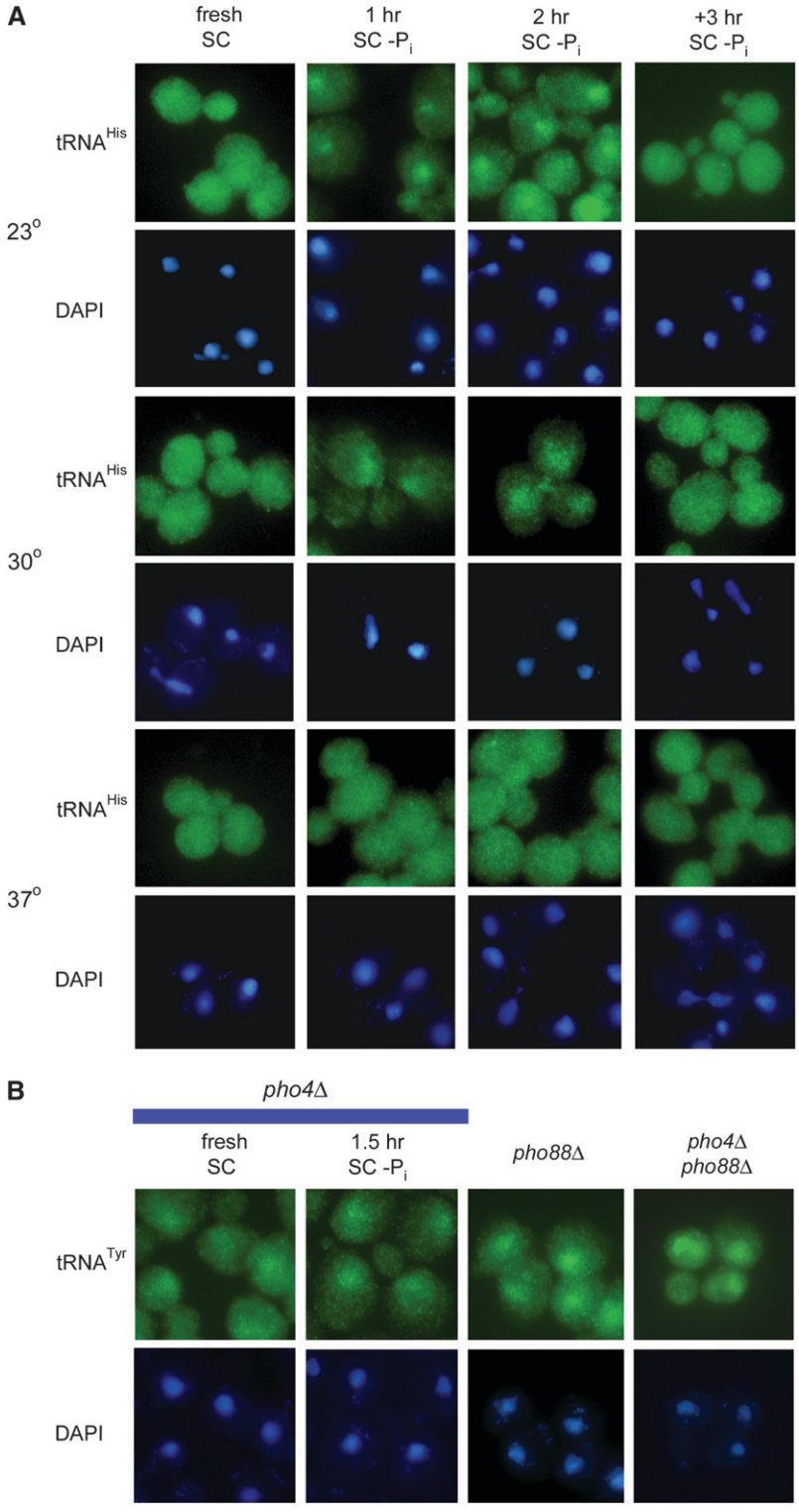

FIGURE 3.—tRNA location within P_i-deprived cells. (A) P_i starvation time course of wild-type cells grown at 23°, 30°, and 37°. BY4742 cells grown in SC (column 1) or SC–P_i (columns 2–4) for the indicated amount of time at 23° (rows 1 and 2), 30° (rows 3 and 4), or 37° (rows 5 and 6) were analyzed by FISH. The cellular distribution of $tRNA^{His}$ is shown (rows 1, 3, and 5). The same cells were stained with DAPI (rows 2, 4, and 6). (B) P_i-starved *pho4*Δ cells and YEPD-grown *pho88*Δ *pho4*Δ and *pho88*Δ cells. Cellular distributions of $tRNA^{Tyr}$ (row 1) determined by FISH, of *pho4*Δ *MAT***a** cells grown in fresh SC or SC–Pi for 1.5 hr, and of *pho88*Δ *MAT***a** and *pho4*Δ *pho88*Δ. Cells were stained with DAPI to reveal the location of DNA (row 2).

reticulum (ER; data not shown). This location is consistent with the results of the genomewide protein localization study that employed C-terminal GFP tags (HUH *et al.* 2003) and the observed membrane association of Pho88 (YOMPAKDEE *et al.* 1996). As Pho88 was located in the ER, it was unlikely to directly bind and transport tRNA from the nucleus to the cytosol. Given that deletion of *PHO88* caused a defect in P_i uptake from media (YOMPAKDEE *et al.* 1996), it was possible that the low intracellular P_i levels caused the tRNA nuclear accumulation. This possibility had precedent as amino acid starvation has been shown to cause tRNA nuclear accumulation (SHAHEEN and HOPPER 2005). If *pho88*Δ cells redistributed tRNA in response to low intracellular

P_i levels, then wild-type cells that cannot import P_i due to lack of substrate should also have tRNA nuclear accumulation.

To address this prediction, wild-type cells (strain BY4742) were grown on synthetic complete media lacking KH_2PO_4 (SC–P_i) for various lengths of time. This approach allowed a controlled starvation period and minimized the risk of suppressor appearance. The cellular distributions of tRNA were then determined by FISH. As expected, $tRNA^{His}$ was evenly distributed in wild-type cells grown in fresh SC media for 2 hr (Figure 3A, column 1). An even distribution of $tRNA^{His}$ was also visible in cells grown for 30 min in SC–P_i (data not shown). Cells grown at 23° in SC–P_i for 1 hr displayed nuclear accumulation of $tRNA^{His}$ (Figure 3A, column 2, row 1) as did cells grown at 30° in SC–P_i for 1 hr (Figure 3A, column 2, row 3). Thus, cells redistributed tRNA in response to P_i removal.

Unexpectedly, tRNA nuclear accumulation in response to P_i deprivation demonstrated temperature- and time-dependent components. While FISH is primarily a qualitative technique, the $tRNA^{His}$ nuclear accumulation in cells grown at 23° reproducibly appeared to be more intense than in cells grown at 30° (Figure 3A, columns 2 and 3, rows 1 and 3). In contrast, cells grown at 37° in SC–P_i did not exhibit nuclear accumulation of $tRNA^{His}$ (Figure 3A, columns 1–4, row 5). When cells were grown at 23° or 30° for 2 hr in SC–P_i, tRNA nuclear accumulation appeared diminished in comparison to the 1-hr time point. Moreover, cells grown for 3.5 or 12 hr in SC–P_i had $tRNA^{His}$ nucleus–cytosol distributions similar to cells grown in fresh SC. The redistribution of $tRNA^{Tyr}$ and $tRNA^{Met}$ in response to growth in SC–P_i mirrored the demonstrated redistribution of $tRNA^{His}$ (data not shown). The data indicated that denying wild-type cells readily available sources of P_i caused temperature-dependent, transient tRNA nuclear accumulation, in contrast to *pho88*Δ cells, which constitutively accumulated tRNA in the nucleus.

Activation of the *PHO* pathway is a well-studied response to P_i deprivation (Carroll and O'Shea 2002). The subcellular location and activity of Pho4p, the master transcription factor of the P_i starvation response, is regulated through phosphorylation at four sites. Pho4 is cytosolic, inactive, and highly phosphorylated when cells are grown in media rich in P_i as the Pho80/Pho85 cyclin–CDK complex is fully active and maintains Pho4 in a highly phosphorlyated state (Carroll and O'Shea 2002). When cells are grown in low P_i medium, the Pho80/Pho85 cyclin–CDK complex is partially inhibited by Pho81, causing Pho4 to be only partially phosphorylated. In this partially phosphorylated state, Pho4 is nuclear and activates the transcription of genes such as Pho84, a high-affinity P_i transporter (50% of maximal expression). Partially phosphorylated Pho4 has a minimal effect upon the transcription of other phosphate-responsive genes, including the acid phosphatase (rAPase), encoded by *PHO5*, which is expressed at 10% of maximum levels (Springer *et al.* 2003). Full inhibition of Pho80/Pho85 by Pho81 in response to P_i deprivation causes Pho4 to become fully dephosphorylated and competent in activating transcription of all its target genes, including Pho5 (Springer *et al.* 2003).

TABLE 3

Acid phosphatase activity

P_i deprivation (hr)	Average[a] (A420/A600)	Standard deviation	% rAPase activity of unstarved cells
0	0.845	0.146	100
2	1.223	0.035	145
3.5	2.350	0.396	278
5	3.707	0.909	439
7	6.827	1.112	808
10	9.294	0.244	1100

[a] Average of four data points.

To ascertain when tRNA nuclear accumulation occurs with respect to the *PHO* pathway-mediated gene expression, we determined the enzymatic activity of secreted Pho5. As the amount of the *p*-nitrophenylphosphate converted to *p*-nitrophenolate is proportional to the amount of Pho5 (Toh-e *et al.* 1973), determining production of *p*-nitrophenolate provides an indirect measurement of Pho5 expression. The rAPase activity was assayed (Byrne *et al.* 2004) using intact, early log-phase wild-type cells (strain BY4742) grown in SC–P_i, which duplicated the growth conditions of 23° cell cultures used for FISH analysis. Cells grown for 2 hr in SC–P_i had 145% of basal activity, whereas cells grown for 3.5 hr in SC–P_i had 278% of basal activity (Table 3). After 10 hr of growth in SC–P_i, cells had 1100% of basal activity (Table 3). The rAPase activity indicates that Pho5 has low levels of expression at the time points when tRNA nuclear accumulation occurs (1–2 hr of P_i deprivation).

Nuclear accumulation of tRNA appears to be an early response to P_i deprivation as it occurs slightly after Pho4p translocation from the cytosol to the nucleus (Kaffman *et al.* 1998) in contrast to the later, strong induction of Pho5p expression (Table 3). To address the possibility that the tRNA nuclear accumulation in response to P_i deprivation could be dependent on the *PHO* pathway, the subcellular tRNA distributions in P_i-deprived and replete *pho4*Δ or *pho81*Δ cells were determined. Unstarved *pho4*Δ cells grown at 23° in fresh SC have a slight accumulation of $tRNA^{Tyr}$ (Figure 3B, column 1). As *pho4*Δ and *pho81*Δ cells grown at 23° in SC–P_i for 1.5 hr also exhibited nuclear accumulation of tRNA (Figure 3B, columns 2 and data not shown), an intact *PHO* pathway is not required for tRNA nuclear accumulation induced by P_i deprivation. In addition, *pho4*Δ *pho88*Δ cells displayed tRNA nuclear accumulation that is similar to the accumulation within *pho88*Δ

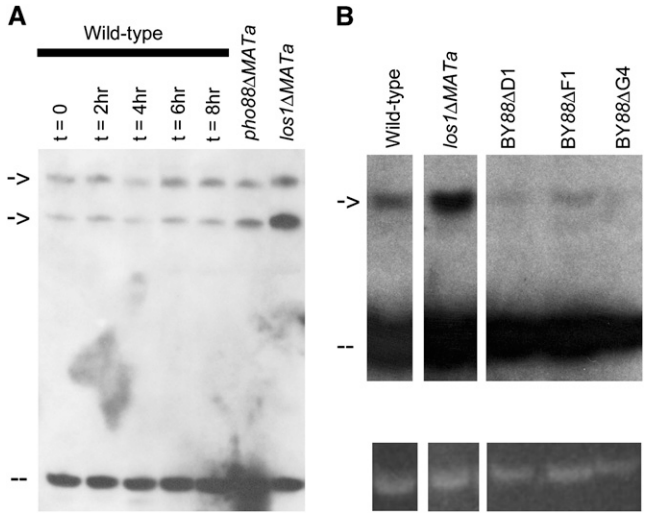

FIGURE 4.—Northern analysis of P_i-starved wild-type cells and *pho88* deletion strains. (A) Samples (10 μg) of small RNAs from BY4741 (wild-type) cells grown in SC (column 1) or in SC–P_i for the amount of time indicated (columns 2–5) at 23° from *pho88*Δ *MAT***a** cells (column 6) and from YD05055 (*los1*Δ) cells (column 7) were separated by electrophoresis and then transferred to a membrane. The membrane was probed with ^{32}P-labeled oligonucleotides complementary to $tRNA^{Ile}$ and detected by autoradiography. Arrows indicate intron-containing pre-tRNAs. Dashes indicate mature tRNAs. (B, top) Samples (10 μg) of small RNAs from BY4742 (wild-type) cells, from YD05055 (*los1*Δ) cells, and from cells of three independently derived *pho88*Δ strains (BY*88*ΔD1, BY*88*ΔF1, BY*88*ΔG4) grown in SC at 23° were separated by electrophoresis and then transferred to a membrane. The membrane was probed with ^{32}P-labeled oligonucleotides complementary to $tRNA^{Tyr}$ and detected by autoradiography. Arrow indicates intron-containing pre-tRNAs. Dashes indicate mature tRNAs. (Bottom) Photo of the ethidium–bromide-stained polyacrylamide gel, prior to transfer, illuminated by ultraviolet light.

cells (Figure 3B, columns 4 and 3, respectively). Therefore, P_i deprivation-induced tRNA nuclear accumulation is an early, signal-mediated response to P_i deprivation that does not require the *PHO* pathway.

Mature tRNA accumulated within nuclei in response to P_i deprivation enter via the retrograde transport pathway: The current model of tRNA nucleus–cytosol transport has two modes for tRNA nuclear egress: primary nuclear export of newly synthesized tRNAs and re-export of mature tRNA. Blocking the primary nuclear export of tRNAs by mutation of *LOS1*, or any other members of the Ran pathway, causes accumulation of intron-containing pre-tRNAs. If P_i deprivation or deletion of *PHO88* caused a block in the primary tRNA nuclear export pathway, then accumulation of intron-containing pre-tRNAs should have occurred. To determine whether tRNA nuclear accumulation observed in response to P_i deprivation and in *pho88*Δ cells occurs due to an inhibition of the primary export pathway or the re-export pathway, tRNA from wild-type cells grown in SC–P_i and *pho88*Δ cells were analyzed by Northern blot analysis. Depriving wild-type cells of P_i did not cause accumulation of intron-containing pre-tRNAs (Figure 4A). The independently derived *pho88*Δ strains did not exhibit accumulation of intron-containing pre-tRNAs (Figure 4). Therefore, mature tRNA had accumulated within nuclei of *pho88*Δ cells and P_i-deprived wild-type cells.

Since Northern analysis indicated that the tRNA nuclear accumulation observed in response to P_i deprivation was not due to impaired export of newly synthesized tRNA, tRNA nuclear accumulation was likely to have occurred through the tRNA retrograde pathway, similar to amino-acid-starvation-induced tRNA redistribution (SHAHEEN and HOPPER 2005). To verify that tRNA retrograde nuclear accumulation occurs during P_i deprivation and when Pho88 is absent, the distribution of $tRNA^{Glu\text{-}D}$ was determined in "wild-type" heterokaryons grown in SC–P_i and in heterokaryons without Pho88. Heterokaryons were generated by mating yeast cells, in which one of the mating types carries a plasmid-expressing $tRNA^{Glu\text{-}D}$ from *Dictyostelium discoideum* and a *kar1-1* mutation (strains MS739 + $tRNA^{Glu\text{-}D}$ or 8MS88-ΔH2D + $tRNA^{Glu\text{-}D}$), with *KAR1* yeast cells (strain BY4741 or BY*88*ΔD1). The *kar1-1* mutation blocked nuclear fusion upon mating and resulted in cells with a shared cytosol and two separate nuclei, where only one nucleus carried the plasmid. If mature tRNA, in response to P_i deprivation, had entered nuclei through retrograde tRNA transport, then all nuclei in a heterokaryon would have accumulated $tRNA^{Glu\text{-}D}$ when grown in SC–P_i. If it is independent of retrograde tRNA transport, then only nuclei that carried the plasmid-expressing $tRNA^{Glu\text{-}D}$ should have accumulated $tRNA^{Glu\text{-}D}$ when grown in SC–P_i.

Heterokaryons grown at 23° in SC–P_i for 1 or 2 hr, or in fresh SC for 2 hr, were subjected to FISH analysis. To quantify the data, heterokaryons were scored by determining if all, some, or none of the nuclei accumulate $tRNA^{Glu\text{-}D}$. Nearly every heterokaryon grown in SC had an even distribution of $tRNA^{Glu\text{-}D}$ throughout the cell (Figure 5A, column 1; Table 4). Of the heterokaryons grown in SC–P_i for 1 hr, 83.5% accumulated $tRNA^{Glu\text{-}D}$ in all nuclei (Figure 5A, column 2; Table 4), 14.4% accumulated $tRNA^{Glu\text{-}D}$ in some nuclei, and 2.1% had no nuclear accumulation of $tRNA^{Glu\text{-}D}$. The majority of heterokaryons grown in SC–P_i for 2 hr still accumulated $tRNA^{Glu\text{-}D}$ in all nuclei (72.7%; Figure 5A, column 3); however, as previously observed in haploid cells (Figure 3), the accumulation was not as prominent as the 1-hr time point and there was an increase in cells that have no nuclear accumulation (17.2 *vs.* 2.1%). The reduction of the total number of cells exhibiting tRNA nuclear accumulation after 2 hr of growth in SC–P_i was expected because the tRNA nucleus–cytosol distribution of wild-type cells returned to an even distribution between 2 and 3.5 hr of growth in SC–P_i. Since $tRNA^{Glu\text{-}D}$ accumulates in all of the nuclei of the majority of P_i-deprived "wild-type" heterokaryons, similar to amino-acid-deprived "wild-type" heterokaryons (SHAHEEN and HOPPER 2005), the tRNA that accumulated in response to P_i deprivation

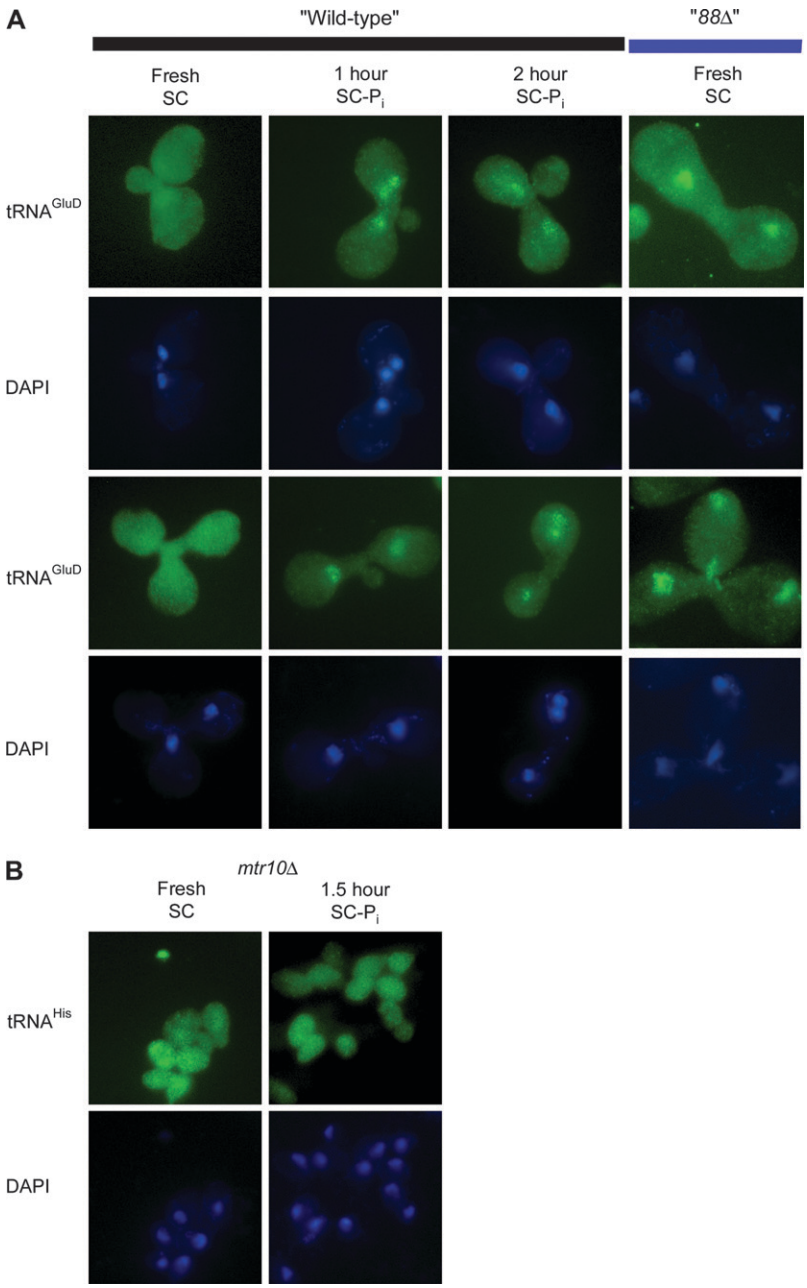

FIGURE 5.—Retrograde transport in *pho88*Δ and P_i-deprived wild-type cells. (A) "Wild-type" heterokaryon cells grown in fresh SC (column 1), SC–P_i for 1 hr (column 2) or SC–P_i for 2 hr (column 3), and "88Δ" heterokaryons (column 4) were analyzed by FISH. (Rows 1 and 2) $tRNA^{Glu\text{-}D}$. (Rows 2 and 4) DAPI stain. (B) *mtr10*Δ *MAT***a** cells grown in fresh SC or SC–P_i for 1.5 hr at 23° were analyzed by FISH. (Row 1) $tRNA^{His}$. (Row 2) DAPI stain.

entered the nucleus via retrograde tRNA transport of cytosolic tRNA.

The anticipated cause of tRNA nuclear accumulation within *pho88*Δ cells was low intracellular levels of P_i caused by defective P_i uptake. Therefore, the tRNA accumulated within the nuclei of *pho88*Δ cells was also expected to have entered the nucleus through retrograde transport. Heterokaryons homozygous for *pho88*Δ ("*88*Δ") were subjected to FISH analysis. Consistent with our prediction, 95.2% of "*88*Δ" heterokaryons accumulated $tRNA^{Glu\text{-}D}$ in all nuclei (Figure 5A, column 5; Table 4). The data indicate that the tRNA accumulated within the nucleus of *pho88*Δ cells entered via retrograde tRNA transport.

Amino-acid-starvation-induced tRNA nuclear accumulation requires the β-importin, Mtr10, as *mtr10*Δ cells exhibit an even distribution of tRNA when grown in SC lacking amino acids (SHAHEEN and HOPPER 2005). If Mtr10 is necessary for P_i-deprivation-induced tRNA nuclear accumulation, then P_i-deprived *mtr10*Δ cells will exhibit an even distribution of tRNA. When grown in SC–P_i at 23° for 1.5 hr, *mtr10*Δ cells showed the same tRNA nucleus–cytosol distribution as *mtr10*Δ cells grown in SC (Figure 5B, columns 2 and 1, respectively). The data indicated that P_i-deprivation-induced tRNA nuclear accumulation was Mtr10 dependent and therefore occurred by a mechanism shared with amino-acid-starvation-induced tRNA nuclear accumulation.

TABLE 4

Heterokaryon assay of tRNA retrograde movement

Cross	Media	PMI	All nuclei accumulate $tRNA^{Glu-D}$ (%)	Some nuclei accumulate $tRNA^{Glu-D}$ (%)	No nuclei accumulate $tRNA^{Glu-D}$ (%)
Wild type	SC	2	0 (0)	1 (1.2)	83 (98.8)
Wild type	SC–Pi	1	81 (83.5)	14 (14.4)	2 (2.1)
Wild type	SC–Pi	2	64 (72.7)	9 (10.2)	15 (17.0)
*88*Δ	SC	2	79 (95.2)	4 (4.8)	0 (0)
88Δ	YEPD	2	36 (97.3)	2 (2.7)	0 (0)

PMI, postmating incubation time.

DISCUSSION

We undertook these studies to systematically query nonessential yeast genes for synthetic interactions with *los1*Δ to learn more about tRNA subcellular dynamics and we discovered a role for the availability of P_i in this process. SGA technology uncovered 131 candidate interactions with *los1*Δ. While 6 candidates were identified in both the 22° and the 37° assays, only 3 (*lrp1*Δ, *rpl13b*Δ, *arc1*Δ) of these had *bona fide* interactions as determined by tetrad analysis and growth assays. Of the 97 candidates evaluated by tetrad dissection, eight novel interactions were uncovered (Table 2). The SGA false-positive rate for *los1*Δ is 90.7% compared to the 25–50% success rate reported for other baits (Tong *et al.* 2004). The false-positive rate of the candidates that appeared in both screens (3 of 6) is 50%. This indicates that many false positives could have been eliminated by repeating the assays at both 22° and 37°. However, we note that *PHO88* would not have been analyzed if SGA had been performed only at 37°. Since we previously noted that amino acid starvation causes tRNA nuclear accumulation (Shaheen and Hopper 2005), one may have expected to uncover *SHR3*, a likely equivalent to Pho88 for amino acid permeases, as a candidate. However, deletion of *SHR3* was inviable by large-scale deletion (Winzeler *et al.* 1999) and was not included in the assay.

The eight novel synthetic interactions uncovered in this study affect amino acid synthesis, translation, mRNA and tRNA processing, and P_i uptake. The variety of cellular processes affected by the identified deletions and the data indicating that some of the identified deletions do not affect tRNA subcellular dynamics, raises the question as to why these synthetic interactions with *los1*Δ occur. *RPL12A* and *RPL13B* encode ribosomal proteins. The synthetic interactions between *los1*Δ and mutations of protein synthesis machinery, including *tef2*Δ and *gcd11* (Hellmuth *et al.* 1998; Grosshans *et al.* 2000), are likely the result of the cumulative impairment of translation by reduced availability of cytoplasmic tRNA (*los1*Δ) and inefficient ribosomes. Aro7 is required for synthesis of tyrosine and phenylalanine. Deletion of *ARO7* affects amino acid synthesis, and reduced amino acid availability may also affect the rate of protein synthesis. The genetic interaction between *lrp1*Δ and *los1*Δ may be caused by multiple defects in cellular RNA levels because previous studies uncovered synthetic lethal interactions between *lrp1*Δ and a variety of genes encoding defective tRNA, mRNA, and rRNA processing activities (Hieronymus *et al.* 2004; Davierwala *et al.* 2005). Our studies uncovered a single synthetic-enhanced growth interaction between *snt309*Δ and *los1*Δ. Since Snt309 is a component of spliceosomes (Chen *et al.* 1999), it is unclear why *snt309*Δ and *los1*Δ would have enhanced genetic interactions.

Different synthetic interactions between *los1*Δ and *pho88*Δ were observed when SGA or direct mutagenesis was employed to generate double mutants. The cold-sensitive nature of the synthetic slow-growth interaction observed in *los1*Δ *pho88*Δ cells may explain why *PHO88* was found as a SGA candidate when the array was performed at 22° but not at 37°. Tetrad dissection was performed at 23° on YEPD medium, which has low levels of P_i (Yoshida *et al.* 1989b). This may have contributed to the absence of *los1*Δ *pho88*Δ progeny. If low temperature and/or medium prevented the appearance of *los1*Δ *pho88*Δ colonies, then tetrad dissection of *pho88*Δ by *los1*Δ crosses on high-P_i medium at 30° may produce *los1*Δ *pho88*Δ colonies. Tetrad dissection also involves a starvation period to induce meiosis, whereas direct mutagenesis occurs on rich media. Thus, it is also possible that *los1*Δ *pho88*Δ spores are unable to germinate after this starvation.

Deletion of *PHO88*, *GTR1*, or *GTR2* caused nuclear accumulation of mature tRNA. Simulating the P_i-uptake defect observed in *pho88*Δ cells by growing wild-type cells in SC–P_i caused transient, temperature-dependent tRNA nuclear accumulation without causing accumulation of intron-containing tRNAs. The data indicate that tRNA nuclear accumulation was not due to impaired export of newly synthesized tRNAs and that P_i-deprived wild-type and *pho88*Δ cells accumulated mature tRNA only in nuclei that entered through tRNA retrograde transport. Consistent with amino-acid-starvation-induced tRNA redistribution, the data also demonstrated that

the tRNA nuclear accumulation observed in P_i-deprived cells was Mtr10 dependent.

Although we have demonstrated that the mature tRNA accumulating within nuclei of *pho88*Δ and P_i-deprived wild-type cells entered the nuclei via the retrograde transport pathway, the mechanism for the accumulation remains unclear. Accumulation could have occurred due to increased retrograde transport, blocked re-export, or simultaneous occurrence of both increased retrograde transport and blocked re-export. Mtr10 may function in a signal transduction pathway regulating retrograde transport and/or re-export or as part of a tRNA importing complex.

Nuclear accumulation of tRNA that occurred due to *PHO88* deletion largely paralleled the accumulation that occurred in P_i-deprived wild-type cells. However, *pho88*Δ cells constitutively accumulated tRNA within nuclei, whereas the accumulation observed during P_i deprivation was transient in nature. This difference may be explained by the differences in how the cells were impaired for P_i uptake. In the absence of Pho88, cells were able to constitutively acquire very low levels of P_i, sufficient for slow growth (Yompakdee *et al.* 1996). In contrast, P_i deprivation caused wild-type cells to undergo a two-phase response. During the first phase, when tRNA nuclear accumulation occurred, polyphosphate is mobilized (Mouillon and Persson 2006), Pho84 is highly expressed, and Pho5 is slightly expressed. The second phase, when tRNA returned to normal distribution, was marked by increased expression of Pho5. Similarly, recent data demonstrated that acute glucose starvation causes tRNA nuclear accumulation, whereas an even distribution of tRNA occurred during prolonged starvation (Whitney *et al.* 2007). This indicates that cells may have acclimatized to prolonged starvation and redistributed previously accumulated tRNA via re-export. Cells with *PHO88* deletions may never reach the extremely low levels of intracellular P_i required for this transition. As P_i-deprivation-induced tRNA nuclear accumulation was independent of Pho4 and Pho81, the signaling pathway(s) controlling tRNA distribution during the P_i deprivation time course have yet to be determined.

Although a goal of this work was to uncover tRNA export pathways that function in parallel to Los1 to export newly synthesized tRNA, such a pathway was not identified. This unidentified exporter(s) may have been missed by SGA or not included in the deletion collection, or it may be encoded by an essential gene that has yet to be recognized as a tRNA transporter. Instead, we successfully uncovered novel connections between *los1*Δ and mRNA processing (*lrp1*Δ) and stable RNA processing (*snt309*Δ) and additional connections to the ribosome (*rpl13b*Δ, *rpl12a*Δ) and amino acid synthesis (*aro7*Δ). The novel synthetic interactions between *los1*Δ and *gtr1*Δ, *gtr2*Δ, or *pho88*Δ identified in this work provided a clear connection between tRNA subcellular dynamics and phosphate availability. Further studies are required to understand the signal transduction and the mechanism by which P_i levels regulate tRNA nucleus–cytosol distribution.

We thank H. Shaheen, M. Whitney, A. Murthi, and K. Stauffer for valuable scientific interactions. This work was supported by a fellowship to R.L.H. from the American Heart Association, by a grant to A.K.H. from the National Institutes of Health, and by grants to C.B. from the Canadian Institute of Health Research, Genome Canada, and Genome Ontario.

LITERATURE CITED

Arts, G. J., M. Fornerod and I. W. Mattaj, 1998a Identification of a nuclear export receptor for tRNA. Curr. Biol. **8:** 305–314.

Arts, G. J., S. Kuersten, P. Romby, B. Ehresmann and I. W. Mattaj, 1998b The role of exportin-t in selective nuclear export of mature tRNAs. EMBO J. **17:** 7430–7441.

Bun-Ya, M., S. Harashima and Y. Oshima, 1992 Putative GTP-binding protein, Gtr1, associated with the function of the Pho84 inorganic phosphate transporter in Saccharomyces cerevisiae. Mol. Cell. Biol. **12:** 2958–2966.

Byrne, M., N. Miller, M. Springer and E. K. O'Shea, 2004 A distal, high-affinity binding site on the cyclin-CDK substrate Pho4 is important for its phosphorylation and regulation. J. Mol. Biol. **335:** 57–70.

Carroll, A. S., and E. K. O'Shea, 2002 Pho85 and signaling environmental conditions. Trends Biochem. Sci. **27:** 87–93.

Chen, H. R., T. Y. Tsao, C. H. Chen, W. Y. Tsai, L. S. Her *et al.*, 1999 Snt309p modulates interactions of Prp19p with its associated components to stabilize the Prp19p-associated complex essential for pre-mRNA splicing. Proc. Natl. Acad. Sci. USA **96:** 5406–5411.

Corbett, A. H., D. M. Koepp, G. Schlenstedt, M. S. Lee, A. K. Hopper *et al.*, 1995 Rna1p, a Ran/TC4 GTPase activating protein, is required for nuclear import. J. Cell Biol. **130:** 1017–1026.

Davierwala, A. P., J. Haynes, Z. Li, R. L. Brost, M. D. Robinson *et al.*, 2005 The synthetic genetic interaction spectrum of essential genes. Nat. Genet. **37:** 1147–1152.

Feng, W., and A. K. Hopper, 2002 A Los1p-independent pathway for nuclear export of intronless tRNAs in Saccharomyces cerevisiae. Proc. Natl. Acad. Sci. USA **99:** 5412–5417.

Goldstein, A. L., and J. H. McCusker, 1999 Three new dominant drug resistance cassettes for gene disruption in Saccharomyces cerevisiae. Yeast **15:** 1541–1553.

Gorlich, D., and U. Kutay, 1999 Transport between the cell nucleus and the cytoplasm. Annu. Rev. Cell Dev. Biol. **15:** 607–660.

Grosshans, H., E. Hurt and G. Simos, 2000 An aminoacylation-dependent nuclear tRNA export pathway in yeast. Genes Dev. **14:** 830–840.

Hellmuth, K., D. M. Lau, F. R. Bischoff, M. Kunzler, E. Hurt *et al.*, 1998 Yeast Los1p has properties of an exportin-like nucleocytoplasmic transport factor for tRNA. Mol. Cell. Biol. **18:** 6374–6386.

Hieronymus, H., M. C. Yu and P. A. Silver, 2004 Genome-wide mRNA surveillance is coupled to mRNA export. Genes Dev. **18:** 2652–2662.

Hopper, A. K., and E. M. Phizicky, 2003 tRNA transfers to the limelight. Genes Dev. **17:** 162–180.

Hopper, A. K., F. Banks and V. Evangelidis, 1978 A yeast mutant which accumulates precursor tRNAs. Cell **14:** 211–219.

Hopper, A. K., L. D. Schultz and R. A. Shapiro, 1980 Processing of intervening sequences: a new yeast mutant which fails to excise intervening sequences from precursor tRNAs. Cell **19:** 741–751.

Huh, W. K., J. V. Falvo, L. C. Gerke, A. S. Carroll, R. W. Howson *et al.*, 2003 Global analysis of protein localization in budding yeast. Nature **425:** 686–691.

Hurt, D. J., S. S. Wang, Y. H. Lin and A. K. Hopper, 1987 Cloning and characterization of LOS1, a Saccharomyces cerevisiae gene that affects tRNA splicing. Mol. Cell. Biol. **7:** 1208–1216.

Kadowaki, T., D. Goldfarb, L. M. Spitz, A. M. Tartakoff and M. Ohno, 1993 Regulation of RNA processing and transport by a nuclear guanine nucleotide release protein and members of the Ras superfamily. EMBO J. **12:** 2929–2937.

Kaffman, A., N. M. Rank, E. M. O'Neill, L. S. Huang and E. K. O'Shea, 1998 The receptor Msn5 exports the phosphorylated transcription factor Pho4 out of the nucleus. Nature **396:** 482–486.

Kutay, U., G. Lipowsky, E. Izaurralde, F. R. Bischoff, P. Schwarzmaier *et al.*, 1998 Identification of a tRNA-specific nuclear export receptor. Mol. Cell **1:** 359–369.

Lagerstedt, J. O., I. Reeve, J. C. Voss and B. L. Persson, 2005 Structure and function of the GTP binding protein Gtr1 and its role in phosphate transport in Saccharomyces cerevisiae. Biochemistry **44:** 511–517.

Martzen, M. R., S. M. McCraith, S. L. Spinelli, F. M. Torres, S. Fields *et al.*, 1999 A biochemical genomics approach for identifying genes by the activity of their products. Science **286:** 1153–1155.

Mouillon, J. M., and B. L. Persson, 2006 New aspects on phosphate sensing and signalling in Saccharomyces cerevisiae. FEMS Yeast Res. **6:** 171–176.

Nakashima, N., N. Hayashi, E. Noguchi and T. Nishimoto, 1996 Putative GTPase Gtr1p genetically interacts with the RanGTPase cycle in Saccharomyces cerevisiae. J. Cell Sci. **109**(Pt. 9): 2311–2318.

Nakashima, N., E. Noguchi and T. Nishimoto, 1999 *Saccharomyces cerevisiae* putative G protein, Gtr1p, which forms complexes with itself and a novel protein designated as Gtr2p, negatively regulates the Ran/Gsp1p G protein cycle through Gtr2p. Genetics **152:** 853–867.

Sarkar, S., and A. K. Hopper, 1998 tRNA nuclear export in Saccharomyces cerevisiae: in situ hybridization analysis. Mol. Biol. Cell **9:** 3041–3055.

Sarkar, S., A. K. Azad and A. K. Hopper, 1999 Nuclear tRNA aminoacylation and its role in nuclear export of endogenous tRNAs in Saccharomyces cerevisiae. Proc. Natl. Acad. Sci. USA **96:** 14366–14371.

Schiestl, R. H., and R. D. Gietz, 1989 High efficiency transformation of intact yeast cells using single stranded nucleic acids as a carrier. Curr. Genet. **16:** 339–346.

Shaheen, H. H., and A. K. Hopper, 2005 Retrograde movement of tRNAs from the cytoplasm to the nucleus in Saccharomyces cerevisiae. Proc. Natl. Acad. Sci. USA **102:** 11290–11295.

Sharma, K., E. Fabre, H. Tekotte, E. C. Hurt and D. Tollervey, 1996 Yeast nucleoporin mutants are defective in pre-tRNA splicing. Mol. Cell. Biol. **16:** 294–301.

Simos, G., A. Segref, F. Fasiolo, K. Hellmuth, A. Shevchenko *et al.*, 1996a The yeast protein Arc1p binds to tRNA and functions as a cofactor for the methionyl- and glutamyl-tRNA synthetases. EMBO J. **15:** 5437–5448.

Simos, G., H. Tekotte, H. Grosjean, A. Segref, K. Sharma *et al.*, 1996b Nuclear pore proteins are involved in the biogenesis of functional tRNA. EMBO J. **15:** 2270–2284.

Springer, M., D. D. Wykoff, N. Miller and E. K. O'Shea, 2003 Partially phosphorylated Pho4 activates transcription of a subset of phosphate-responsive genes. PLoS Biol. **1:** E28.

Stanford, D. R., M. L. Whitney, R. L. Hurto, D. M. Eisaman, W. C. Shen *et al.*, 2004 Division of labor among the yeast Sol proteins implicated in tRNA nuclear export and carbohydrate metabolism. Genetics **168:** 117–127.

Takano, A., T. Endo and T. Yoshihisa, 2005 tRNA actively shuttles between the nucleus and cytosol in yeast. Science **309:** 140–142.

Toh-e, E. A., Y. Ueda, S. I. Kakimoto and Y. Oshima, 1973 Isolation and characterization of acid phosphatase mutants in Saccharomyces cerevisiae. J. Bacteriol. **113:** 727–738.

Tong, A. H., M. Evangelista, A. B. Parsons, H. Xu, G. D. Bader *et al.*, 2001 Systematic genetic analysis with ordered arrays of yeast deletion mutants. Science **294:** 2364–2368.

Tong, A. H., G. Lesage, G. D. Bader, H. Ding, H. Xu *et al.*, 2004 Global mapping of the yeast genetic interaction network. Science **303:** 808–813.

Weis, K., 2003 Regulating access to the genome: nucleocytoplasmic transport throughout the cell cycle. Cell **112:** 441–451.

Whitney, M. L., R. L. Hurto, H. H. Shaheen and A. K. Hopper, 2007 Rapid reversible nuclear accumulation of cytoplasmic tRNA in response to nutrient availability. Mol. Biol. Cell (in press).

Winzeler, E. A., D. D. Shoemaker, A. Astromoff, H. Liang, K. Anderson *et al.*, 1999 Functional characterization of the S. cerevisiae genome by gene deletion and parallel analysis. Science **285:** 901–906.

Yompakdee, C., N. Ogawa, S. Harashima and Y. Oshima, 1996 A putative membrane protein, Pho88p, involved in inorganic phosphate transport in Saccharomyces cerevisiae. Mol. Gen. Genet. **251:** 580–590.

Yoshida, K., Z. Kuromitsu, N. Ogawa and Y. Oshima, 1989a Mode of expression of the positive regulatory genes PHO2 and PHO4 of the phosphatase regulon in Saccharomyces cerevisiae. Mol. Gen. Genet. **217:** 31–39.

Yoshida, K., N. Ogawa and Y. Oshima, 1989b Function of the PHO regulatory genes for repressible acid phosphatase synthesis in Saccharomyces cerevisiae. Mol. Gen. Genet. **217:** 40–46.

Yoshihisa, T., K. Yunoki-Esaki, C. Ohshima, N. Tanaka and T. Endo, 2003 Possibility of cytoplasmic pre-tRNA splicing: the yeast tRNA splicing endonuclease mainly localizes on the mitochondria. Mol. Biol. Cell **14:** 3266–3279.

Communicating editor: S. Sandmeyer